LIP-STUDENTS-20-11

# Muography of a building

Luís Amorim[1,a] and Magda Duarte[1,b]

[1] *Universidade do Minho, Braga, Portugal*

Project supervisors: R. Sarmento, S. Andringa

*October 2020*

**Abstract.** An analysis of the data from a muon detector was performed in order to get a reconstruction of the structure of a building using muography. The muon fluxes for different trajectories were calculated and scrutinized using different strategies and a study of the detector's efficiency was also performed. The project was developed for four months, from June to October. Despite not obtaining a final image of the building, it was possible to reach reality-according and hope-lifting results that motivate us to continue with the project.

KEYWORDS: Particle detector, Efficiency, Muon flux

## 1 Introduction

Muons (with energies of GeV to TeV) are produced in the Earth's atmosphere by the interaction of high energy cosmic rays. Being elementary particles similar to the electron, they have an electric charge of $-1e$ and a spin of 1/2 but hold a much greater mass (about two hundred times the mass of the electron). They are unstable subatomic particles with a mean lifetime of $2.2\,\mu s$ but are able to reach the Earth's surface due to relativistic time dilatation [1].

For this project, the most important muon property is their low interaction with matter, which allows for them to travel great distances in a straight line. This property is, in part, due to their great mass, which leads to muons being subject to smaller accelerations, and to their large energies. Altogether, this allows for muons, when compared to other particles, to penetrate far deeper into matter (in this case the matter of the walls and ceilings of the building) without getting deviated, making it possible for a detector below a considerable amount of dense matter to still record them.

### 1.1 Muography

Muography, as mentioned, is the technique in which this project is based. It was used in the near past and is still used in current days as a modern imaging process that produces a projection of a target volume, in our case a building, by detecting muons either electronically or chemically. These detectors work in such ways – discussed in subsection 1.3 - that is possible to reconstruct the muons' trajectories. An example of an application of muography is the discovery of hidden chambers inside the Giza pyramids in Egypt: a temperature variation built up suspicions about their existence, which was later corroborated using this technique [2].

Even with a low interaction probability, some of the muons will still be stopped when crossing a long path in high density matter. That being said, it is obviously expected that more muons will reach the detector if they come from a path (direction) along which they only have to go across the atmosphere versus a path along which they must travel through a building. The differences in the number of muons that come from the alternative paths will, therefore, hint about the structure that surrounds the detector and eventually produce a muogram, then converted to an "image" called a muograph. All in all, muography is a method similar to radiography but capable of studying much larger objects and the goal that this project was set out to reach was to apply this technique to a building.

### 1.2 The building

The structure under study in this project is the building where the Physics Department of University of Coimbra and the LIP node in Coimbra are based - see Figure 1.

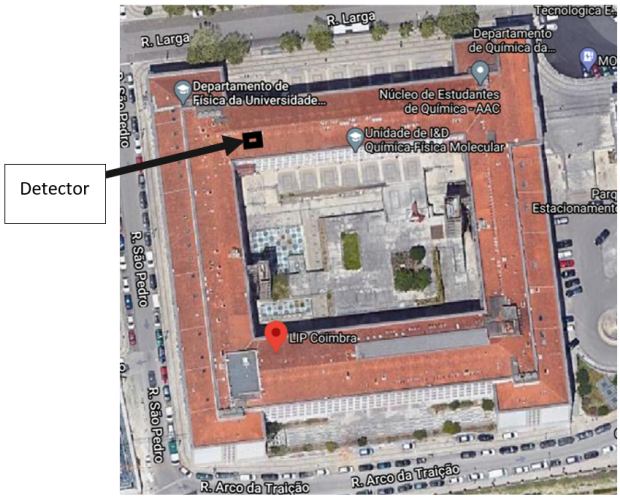


Figure 1: Satelite view of the building and relative location of the detector, marked with a black square [3]

The building has 7 floors, 2 underground, which will be referred to as caves, and 5 identical above ground floors. For simplicity purposes some of the features of the building resulted from assumptions:

- The only walls taken into account for the modeling of the building performed - see section 4 - were the outer exterior walls;

[a] e-mail: a92832@alunos.uminho.pt
[b] e-mail: a89144@alunos.uminho.pt

- The walls were taken has having the same width as the thinnest ceilings: 36 cm;
- The floors' height was considered to be 4 m.

### 1.3 The detector

The detector used consists of a RPC (Resistive Plate Chamber) muon detector [4]. It was built in the LIP Detector Laboratory in the end of 2019 precisely with the purpose of muography.

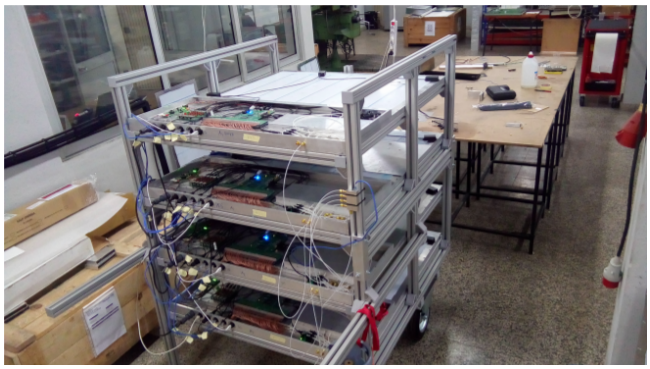

Figure 2: Picture of the muon detector.

It consists of four planes of identical RPCs, each 1 squared meter, read in 64 channels. Muons ionize the gas, and produce a localized charge avalanche. The charge detected in each pad/channel is registered, giving access to the muon passage point in that plane. Since there are multiple planes, if a muon is detected in more than one, we can access the corresponding passage channels as coordinates and reconstruct the trajectory of the particle, as shown in Figure 3.

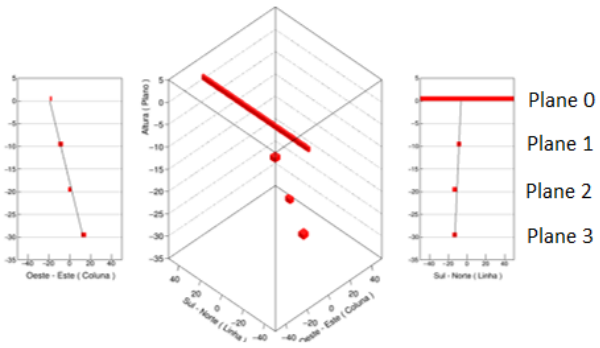


Figure 3: Example of the reconstruction of a muon trajectory.

The top plane, plane 0, has columned channels - see Figure 4a - while the remaining three present a more complex configuration, having a squared central region - the corepix - with small channels (3.8 cm × 3.8 cm) that allow for great precision on the determination of the passage coordinates and, consequently, on the determination of the trajectories of the muons - see Figure 4b. Given the degree of detail provided by the corepix, plane 0 and remaining regions of planes 1, 2 and 3 were disregarded as for a first analysis.

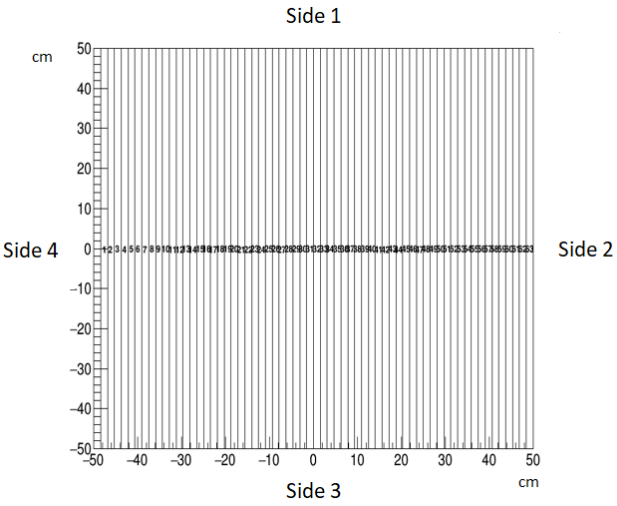


(a)

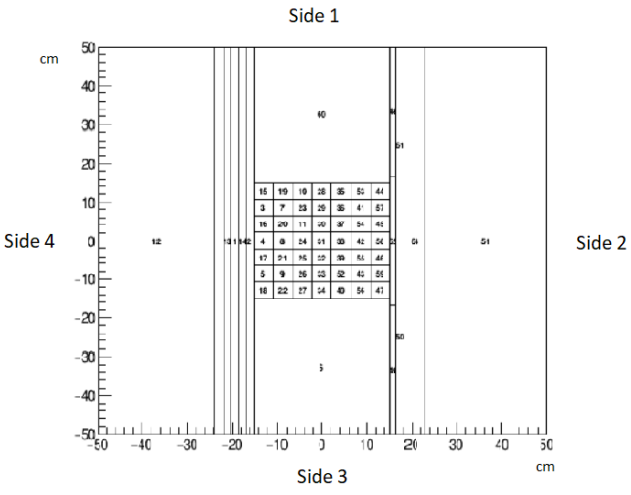


(b)

Figure 4: (a) Configuration of the top plane of the detector, plane 0. (b) Configuration of the bottom three planes of the detector, planes 1, 2 and 3.

## 2 Data

An event, once registered, offers the following high-level information:

- Time at which it occurred: data and hour;

- Channel through which the muon went through in each plane of the detector, which is taken as being the one with highest charge;
- Corresponding line and column of the channel.

### 2.1 Filtering

In order to work with data that was in accordance with the muon properties previously pointed out and that provided useful information from the calculation of trajectories perspective, the following criteria was established:

- there were two trigger planes: the event was only accounted for when there was a signal on both of the previously defined trigger planes. In order to be registered, the time interval between the passage of the muon on the two planes had to be within 30 ns;
- the muon had to surpass the bottom three planes on the central region, the corepix;
- the path reconstructed for the events had to be consistent with a straight line trajectory: taking planes 1 and 3 registered channels, one considers the 16 alternative trajectories that come from taking the straight lines that link the corners of the channels - this approach is taken because the precise passage point within a channel is not known. It's then possible to determine the channels that would make sense for the muon to go through in plane 2 (the multiple channel possibilities that sometimes arise from a muon supposedly landing mid-channels were taken into account).

### 2.2 Data sets

Throughout this internship 4 sets of data from March, June, August and September have been analyzed.
Between these acquisition periods, modifications have been made to the localization, orientation and configuration of the detector in order to not only obtain more information and perform counter-analysis, but also to study the performance of the detector itself.

For the four months the detector was moved around only in LIP's detector laboratory in cave -1. However, even in this room, the conditions to which it was subjected varied, as there are regions of it, namely the one where the detector was in September, not surrounded by as much matter. This is due to the fact that, on the floors above, the corresponding areas are already the outdoors of the building, as Figure 5 tries to portrait.

Despite the changes, in order to make the analysis simpler, the detector's geometry was played as an advantage, by always having its sides aligned with the four sides of the building.

Tables 1 and 2 and Figure 5 summarize the different settings of the detector:

Table 1: Localization of the detector.

| Month | Unit ceilings[1] above the detector | Relative orientation[2] | Wall distance to the side[3,4] (m): | | | |
|---|---|---|---|---|---|---|
| | | | 1 | 2 | 3 | 4 |
| March | 7 | ↑ | 7 | 63 | 5 | 25 |
| June | 7 | ↑ | 7 | 63 | 5 | 25 |
| August | 7 | ← | 27 | 7 | 61 | 5 |
| September | 2 | ↑ | - | - | 2 | 6 |

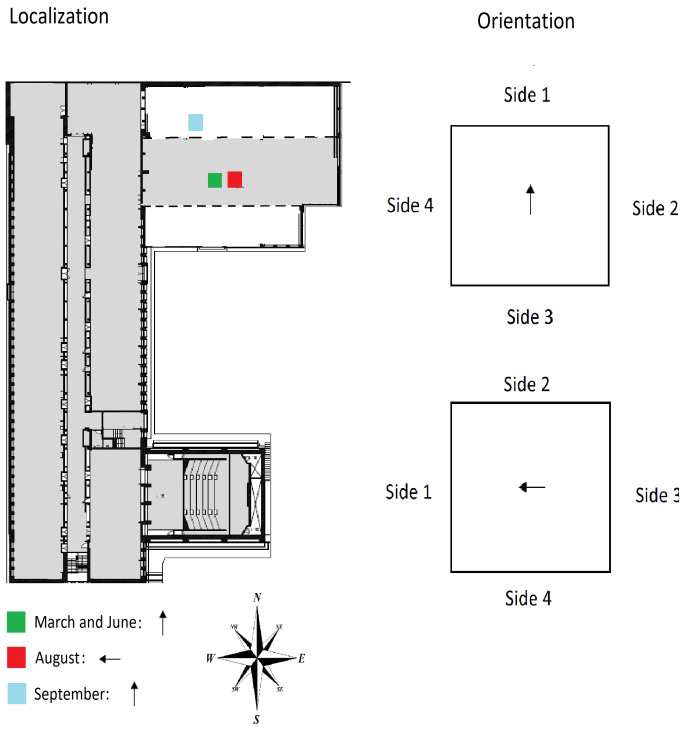


Figure 5: Partial scheme explanatory of the detector's localization and orientation through the months. In grey are the areas which exist in the above ground floors and in white the ones that are only part of the building for the two caves. Figure not to scale.

[1] A unit ceiling is defined as a ceiling with 36 cm of width. Therefore, $n$ unit ceilings above a certain floor means that, given the number of ceilings above that floor and their width, there are about $n \times 36cm$ of "ceiling material" on top of that floor. This correspondence will turn out to be useful on section 3.

[2] In ← relative orientation the detector is rotated 90º in comparison to ↑ orientation.

[3] Wall distance to the side: surmise about the distance between the exterior building's wall correspondent to the side of the detector.

[4] Sides of the detector are defined on Figures 4a and 4b.

Table 2: Configuration of the detector.

| Month | Planes displacement (cm) | Trigger planes | HV[5] automatic regulation |
|---|---|---|---|
| March | 14.5 | 1 and 3 | Off |
| June | 14.5 | 1 and 2 | On |
| August | 29.5 | 1 and 2 | On |
| September | 29.5 | 1 and 2 | On |

## 3 Detector Efficiency and Uniformity

Working with a relatively new detector going through adjustments brings the urge to follow the evolution of this instrument and its reliability. That's where the efficiency study comes into place.
For data having non-consecutive trigger planes there is a direct way of calculating the efficiency of the free plane, analysed in subsection 3.1. However, the data sets resulting of a different trigger configuration, one with consecutive trigger planes, requires a more intricate and not straightforward alternative method, which is studied in subsection 3.2.

### 3.1 Direct measurement of pad efficiency

In March, the trigger planes were planes 1 and 3 - review Table 2. This configuration leads to an obvious measurement of the well-functioning of plane 2: events that surpass planes 1 and 3 in the same pad, as they define vertical muons, should go through the same pad in plane 2. Then, efficiency of a channel $i$ by this method, $\epsilon_1[i]$, is to be calculated with the following formula:

$$\epsilon_1(i) = \frac{s123[i]}{s13[i]} \tag{1}$$

where

- $s123[i]$ is the number of events that go through the same channel $i$ in planes 1, 2 and 3;
- $s13[i]$ is the number of events that go through the same channel $i$ in planes 1 and 3.

Figures 6 and 7 constitute the study performed on this efficiency calculation method.

[5]HV stands for High Voltage, which is an aspect of the configuration of the detector and on which the RPC efficiency depends, as well as on environment temperature and pressure. From June on, this feature, the HV, is automatically adjusted to compensate the environmental factors and provide a stable (and high) efficiency as it will be noticeable in section 3.

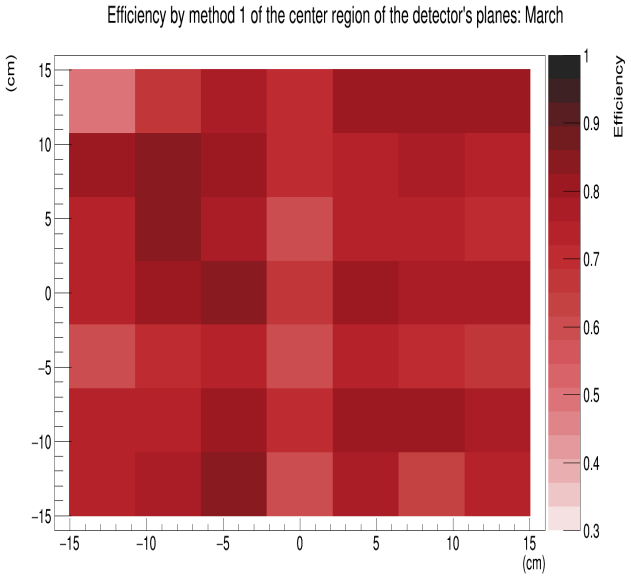


Figure 6: Mapping of $\epsilon_1$ in the detector's central region in March.

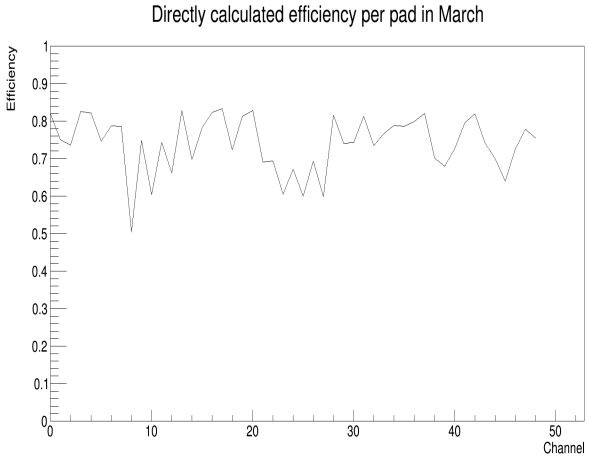


Figure 7: $\epsilon_1$ over the central region for the month of March.

The mapping of $\epsilon_1$ for the whole month - Figure 6 - as well as the graphic correspondent - Figure 7 - raises a uniformity problem associated with the detector. The variation of efficiency across the corepix is considerable, as it can take values of 0.50 up to 0.83. This is an important characteristic for the study of the building's structure, for some muons' directions may be biased due to the detector not being uniform, possibly resulting in misleading conclusions. In any case, during March the detector was still not in a stable operative mode and the dedicated background studies in these data might improve the situation.

### 3.2 Vertical transmission and indirect calculation of effiency

In June, August and September, the trigger planes were 1 and 2 - review Table 2. If method 1 was still to be applied

to find out the efficiency of plane 3, for this is the free plane now, one would need to have into account the fact that muons going through planes 1 and 2 in the same channel are not to surpass plane 3 in the same channel mandatorily. The following method, independent of the trigger planes, then becomes clearer, not requiring geometric factors to come into place, as the adaptation of the direct approach would. However, in the first place, the determination of two parameters is necessary: the vertical transmission and the vertical muon rate expected in one pad of the corepix.

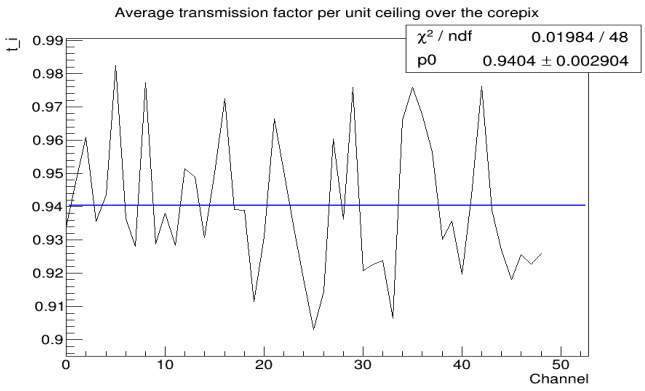


Figure 8: $t$ per pad and average over the corepix.

### 3.2.1 Vertical Transmission

The vertical transmission, $T$, is defined as the fraction of vertical muons that, having reached the top of the building, are still transmitted all the way to the detector: it varies according to the number of unit ceilings above the region where the detector is located. For this reason, considering that this parameter changes for the month of September - review Table 1 - a general measuring unit is required.

In order to achieve that unit, one assumption was made in the first place and later verified to be reasonable using Monte Carlo simulation: the curve of vertical muons reaching each floor is an exponential or, equivalently, the percentage of muons transmitted through the same amount of matter is constant. Consequently, the unit ceilings are "additive", meaning that an equal transmission factor acts on the muons in each unit ceiling, for they are defined as being the same amount of matter. Therefore, one can define the needed general unit: $t$, the transmission factor associated with a unit ceiling. Having this and the localization of the detector in mind for the months of August and September - review Table 1 - one gets a transmission $T$ equal to $t^7$ and $t^2$, respectively.

Given the fact that the detector holds the same configuration for both of these months - review Table 2 - and that its efficiency didn't suffer great change[6], the difference between the number of vertical muons being measured by the detector will only be due to the transmission having changed ($T = t^7 \rightarrow T = t^2$). Performing the quotient between the maps of vertical rates of September and August should result in a uniform distribution of

$$\frac{t^2}{t^7} = t^{-5}$$

which we power to $-\frac{1}{5}$ in order to get $t$. Calculating its average over the corepix - see Figure 8 - one finally gets $\hat{t} = 0.940 \pm 0.003$. This value was verified to be compatible with Monte Carlo expectation for 36 cm ceiling at 82.8 $g/cm^2$.

[6]This inference comes from the simple fact that no alterations were performed between these months.

### 3.2.2 Expected vertical muon rate per pad

For the new approach of calculating the corepix efficiency another parameter, besides the transmission, is needed: the vertical muon rate expected in one pad of the detector, with the premise of it being located in the exterior, $f^{vert}_{E_{theo}}$.

One knows that the nominal value for the muon flux at the Earth's surface is of 130 muons/s/m$^2$ [1]. Given this value, to obtain $f^{vert}_{E_{theo}}$, the area correspondent to one pad and the solid angle covered by it, directly linked to the detector's acceptance, must be calculated. While the area of one pad is constant, its acceptance will change according to the planes displacement: if the planes are more spaced out, the pad's "vision", in terms of what muons' directions it's able to see, will funnel.

Besides these parameters, two considerations are still to be made:

- There is a known $\cos\theta$ dependence of the open air flux of cosmic ray muons;
- There is a $\cos\theta$ dependence of the effective (projected) pad area.

As to calculate $f^{vert}_{E_{theo}}$ with more accuracy, given its multiple dependencies, we recurred to a Monte Carlo simulation.

Having both of these results, the vertical transmission and the expected vertical muon rate in one pad, which are specified for the different months in Table 3, one is ready to take the indirect calculation of efficiency.

### 3.2.3 Indirect calculation of efficiency

Assuming that the 3 bottom planes have equal efficiency, a comparison between the expected rate of vertical muons in one pad $i$ and the experimental one leads to the efficiency of the channel $i$, $\epsilon_2[i]$:

$$\epsilon_2(i) = \sqrt[3]{\frac{f^{vert}_{meas}[i]}{f^{vert}_{theo}}} \quad (2)$$

where

- $f^{vert}_{meas}[i]$ is the experimental rate of vertical muons on channel i;

• $f^{vert}_{theo}$ is the expected rate of vertical muons on a channel.

Since $f^{vert}_{meas}[i]$ is obtained from the data by simply dividing the number of vertical muons crossing pad $i$ by the acquisition time, there's left to be determined the denominator, which is logically given by:

$$f^{vert}_{theo} = T \times f^{vert}_{E_{theo}} \tag{3}$$

Since these are the parameters studied previously, the analysis of the efficiency calculated indirectly can be performed without further side notes - see Figures 9 and 10.

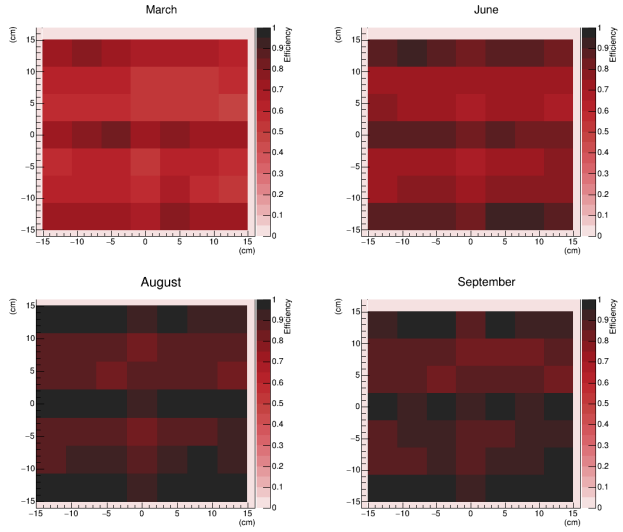


Figure 9: Mapping of $\epsilon_2[i]$ for the different acquisition periods.

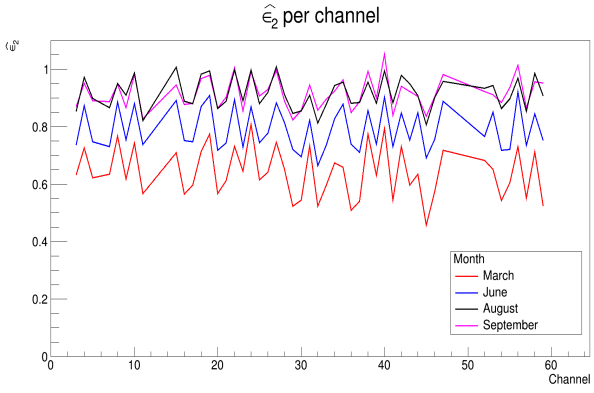


Figure 10: $\hat{\epsilon}_2[i]$ per pad for the different acquisition periods.

With the mapping of $\hat{\epsilon}_2$ and the respective graphic, not only the continuous lack of uniformity on the corepix throughout the months is clear, as the analysis with the direct measurement of efficiency had already pointed out, as a pattern becomes now evident: there are three lines that seem to be preponderant to detect more events: the top, center and bottom ones. This raises, again, the concern about biased data being collected by the detector. One can try to work with this pattern, however, it's important to first determine whether its impact is sufficient to overlap any results that are found or not. This uniformity problem has been and will continue to be studied so as to determine its origin and try to eliminate it.

That being said, the attenuation of the pattern throughout the months is a positive evolution that should be pointed out.

### 3.3 Average efficiencies

Having both forms of calculation of efficiency, direct and indirect, one may now proceed to not only evaluate the time-evolution of the detector, but also to compare the methods - Figure 11 and Table 3.

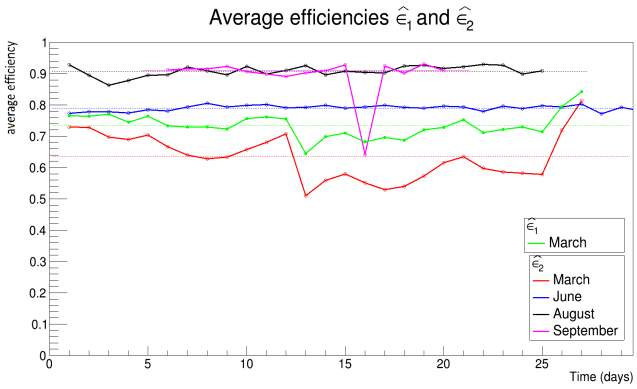


Figure 11: Evolution of $\hat{\epsilon}_1$ for March and of average $\hat{\epsilon}_2$ for the 4 acquisition periods.

Table 3: Average efficiencies and respective parameters used for the indirect calculation - $T$ and $f^{vert}_{E_{theo}}$ ($\times 10^{-3}$ muons/s).

| Month | $\hat{\epsilon}_1$ | $T$ | $f^{vert}_{E_{theo}}$ | $\hat{\epsilon}_2$ |
|---|---|---|---|---|
| March | 0.735 ± 0.007 | 0.65 ± 0.01 | 2.0 ± 0.2 | 0.634 ± 0.014 |
| June | - | 0.65 ± 0.01 | 2.0 ± 0.2 | 0.790 ± 0.002 |
| August | - | 0.65 ± 0.01 | 3.9 ± 0.4 | 0.908 ± 0.003 |
| September[7] | - | 0.884 ± 0.006 | 3.9 ± 0.4 | 0.912 ± 0.003 |

Firstly, it is to notice a discrepancy between the values of $\hat{\epsilon}_1 = 0.735 \pm 0.007$, - found in subsection 3.1 - and $\hat{\epsilon}_2 = 0.634 \pm 0.014$, both respective to March. It potentially reveals that the assumption that the 3 bottom planes share the same efficiency, in which $\epsilon_2$ calculation is based at, is not correct and that, therefore, an independent method of assessing each planes' efficiency may be required. Nonetheless, $\hat{\epsilon}_2$ can still provide information about the detector's improvement, if it is the case.

Analysing the evolution of the values obtained for $\hat{\epsilon}_2$ for the different months, the increasing of the efficiency stability and modulus, $\hat{\epsilon}_2 = 0.634 \pm 0.014 \rightarrow \hat{\epsilon}_2 = 0.912 \pm$

[7] For the calculation of $\hat{\epsilon}_2$ of September, data from day 16 was disregarded, as maintenance was ocurring during this day.

0.003, is notorious, reaching the values for which RPC's efficiency is known for of about 90%[4].

The first growth from March to June, $\hat{\epsilon_2} = 0.634 \pm 0.014 \rightarrow \hat{\epsilon_2} = 0.790 \pm 0.002$, came from the automatic regulation of HV, according to temperature and pressure, that started happening from June on - review Table 2 - as one can point out that the variations once spotted in March are non existing for June. The increase from June to August, $\hat{\epsilon_2} = 0.790 \pm 0.002 \rightarrow \hat{\epsilon_2} = 0.908 \pm 0.003$, although not studied in a thorough way, may have come from the detector having been moved to a movable structure, which possibly altered the detector's efficiency.

As for the values presented for August, $\hat{\epsilon_2} = 0.908 \pm 0.003$, and September, $\hat{\epsilon_2} = 0.912 \pm 0.003$, one could argument that their similarity comes from the fact that one of the parameters used for the calculation, the vertical transmission $T$, was calculated at the quotient of these months' data expense. However, given the validation of the value of the transmission with a Monte Carlo simulation, as previously mentioned, and given the unchanged patterns seen with "rawer data" (not worked through with $T$), that concern becomes invalidated. All things considered, one notices that, similarly to June, during these last two months the detector's efficiency is characterized by a great stability, with the exception of September 16, during which the detector was under maintenance.

# 4 Modeling of the building

After filtering the data, we proceeded to relate it to the building's structure. So as to have a preliminary idea of what is expected in terms of the building's interference with the different trajectory muons, a modeling of the building is required. The first task is to choose a reference frame in order to define the muons' trajectories.

## 4.1 Defining Angles

In order to describe the trajectory of a muon two angles are defined, the **zenith angle (theta-$\theta$)** and the **azimuth angle (phi-$\phi$)**. These angles are important to define the side of the building the muons come from and the angle of incidence.

**Angle** ($\theta$) - the zenith angle is the angle between the trajectory line and the vertical axis, that is, the angle of incidence in the building according to the vertical reference, Z axis;

**Angle** ($\phi$) - the azimuth angle is the angle corresponding to the "side" / the horizontal direction the muons come from. It is measured by the position change in the xOy plane.

These angles are calculated with simple trigonometry knowing the channels through which the muons passed on planes 1 and 3. As it is not possible to know the exact position at which the muon crossed a pad, for the angles calculation, one uses the center of the pad as a reference point.

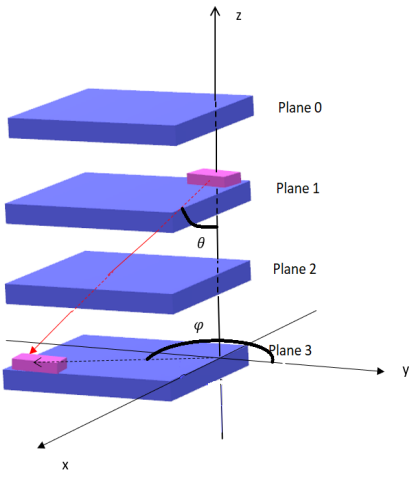


Figure 12: Trajectory angles definition.

## 4.2 Distance travelled through matter

After defining the trajectories, one may proceed to calculate the matter travelled according to the different trajectories. An equivalent analysis is Figure 13: the plot of the difference in the number of walls and ceilings that a muon goes through depending on the angles of its trajectory.

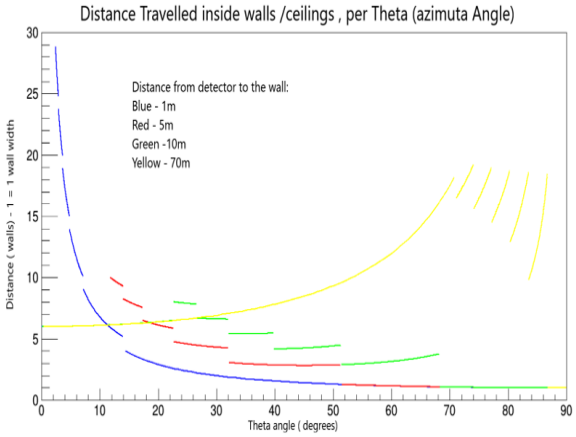


Figure 13: [8]Distance travelled inside walls/ceilings, per Theta for different Phi's.

## 4.3 Reductions in flux: damping

After studying how the distance travelled inside matter varies with the angles, we established a relationship of the distance travelled with the attenuation expected in the muon flux. The correspondence being made is, basically, as simple as saying that a smaller flux is expected for angles at which the muons have to cross more matter. If, for

[8]In this figure, the values taken for the distances of the detector's sides to the walls are merely illustrative and were chosen so as to study borderline cases that are not completely discrepant of the order of magnitude of the real ones.

a certain trajectory, the muons cross less matter we expect a bigger muon flux for the respective azimuth and zenith angle of that trajectory. So, the differences expected on the muon flux are calculated according to the walls and ceilings travelled, which is studied in subsection 4.2.

In a simple way, a calculation of what is the reduction, "the damping effect", produced by a ceiling/wall on the muon flux is made:

- from the analysed data for vertical events, one knows that after crossing 1 ceiling the muon flux is only 94% of the value measured outside. Adjusting this to an exponential law we can obtain the damping factor

$$D(1) = e^{-1/\lambda} = 0.940 \implies \lambda = 16.2\,\text{ceilings}\,. \quad (4)$$

So the general formula for the decay of the muon flux, $D$, as a function of the number of walls/ceilings crossed by the muons, $d$, is

$$D(d) = e^{-d/16.2}\,. \quad (5)$$

Using this function combined with the number of ceilings/walls for the different directions, which was already encountered in Figure 13, one reaches Figure 14.

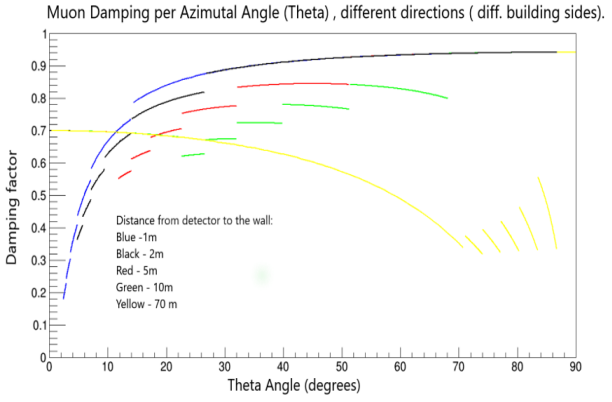


Figure 14: Attenuation in the muon flux per Theta.

Having reached a model for the 4 sides of the building, one can, following the same theory, extend it to a 2D model. In Figure 15 that approach is performed so as to know the expected quotient of rates between August and September.

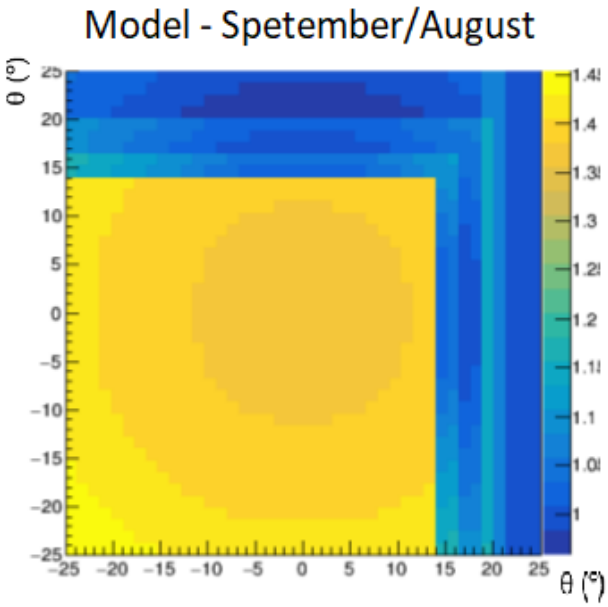


Figure 15: [9]2D model of the building's attenuation for the quotient September/August.

## 5 Data study strategies

### 5.1 Overall view

An approach to extrapolate the building's structure may be to identify discrepancies between the number of muons reaching the detector from all the possible directions that one can study with the correspondent detector's configuration. Following this strategy, we can adopt the following representation: a histogram that tracks record of the muon rate distribution in all of those directions. This representation is exemplified for the months of August and September in Figures 16a and 16b respectively. To explain what each bin represents, take the central one: its color quantifies the rate of vertical events in the given period of acquisition; as for the bin immediately to its right, it quantifies also the muon rate but of muons that, having travelled from plane 1 to plane 3 and moved one column to the right, remained in the same line of channels and so on. To sum up, the histogram is a measurement of the muon rate in particular directions, being the relative localization of a bin defining of what particular direction the bin is a representation of. To this form of visualization we called "Overall view".

[9]Work is still being developed so as to improve this model, namely, measurements of the building so as to be able to perform a direct comparison of the model with the results. As is has been mentioned, so far, information such as the floors' height and the walls' width have only resulted from assumptions. Moreover, an important characteristic of the building hasn't been yet taken into account, as it will become clear in the assessing of the data in section 5.

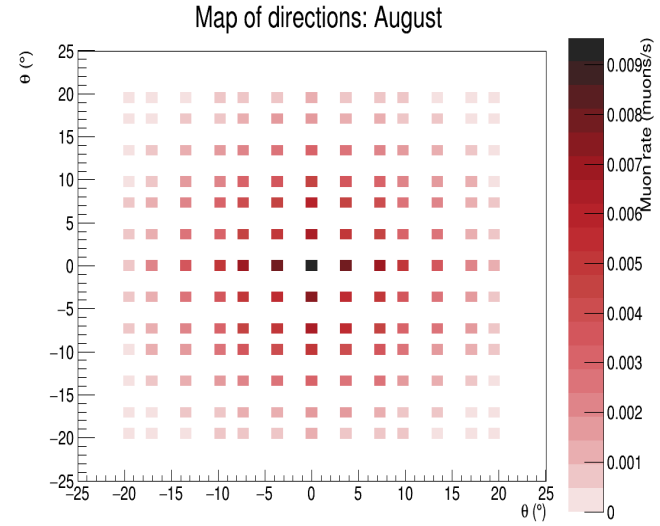


(a)

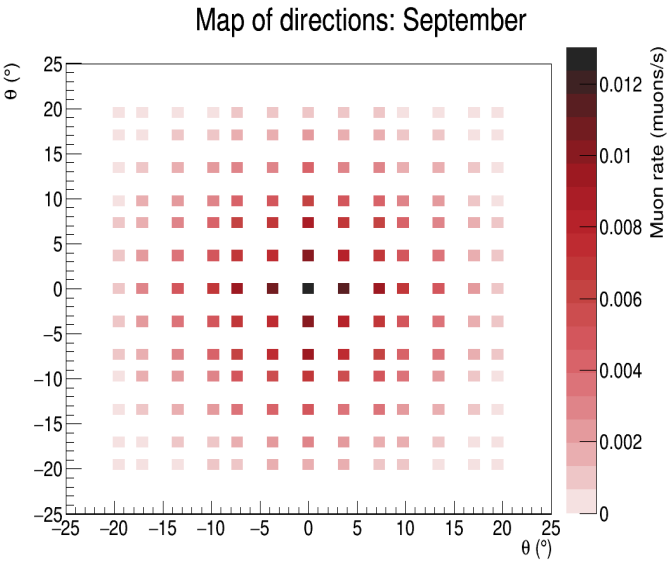


(b)

Figure 16: [10](a) "Overall view" for August data. (b) "Overall view" for September data.

As one finds out about the efficiency pattern on the corepix - review Figure 9 - a problem that biases the interpretation of transmission muography data arises. However, though the endurance of this pattern is worrying, it allows for one to cancel it recurring to the August and September data: the average efficiency between these months didn't suffer great change - see Table 3 - for what, if one performs the quotient between those sets of data, the efficiency patterns will cancel out. Thus, the quotient between the September and August "Overall View" histograms is performed - see Figure 17.

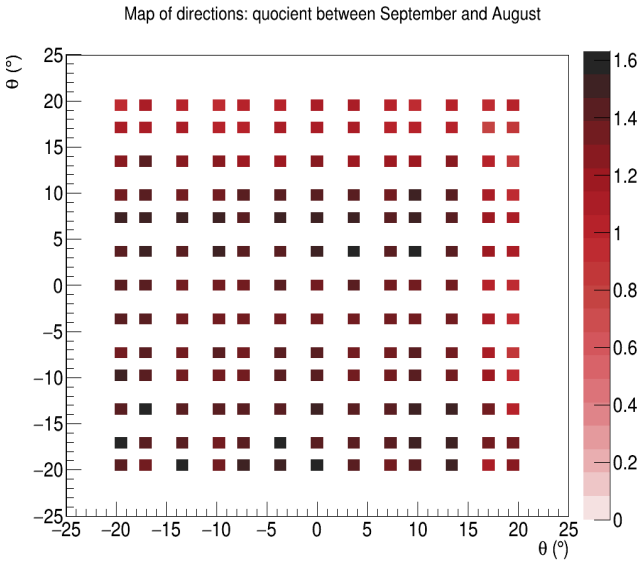


Figure 17: Quotient between September and August's "Overall view".

From Figure 17, a difference between the rates of the set of top and right bins and the rates of the set of bottom and left bins is noticeable. Being aware of the changes in the detector's orientation and localization from August to September - review Figure 5 and Table 1 - one can argument that this discrepancy is actually representative of the two walls closer to the detector in the month of September.

In August, the detector's localization sets it up in such a way that it is surrounded with the 4 exterior walls all throughout the above ground floors, while in September, only 2 walls remain "surrounding" the detector in the above ground floors. Therefore, a more uniform distribution is expected for August, while for September clear asymmetries should appear. So, discrepancies in the quotient should be caused by the September data. If we review the orientation for the month of September, one sees that the two sides of the detector opposite to the walls are 1 and 2, therefore, less muons are expected to reach the detector if they come from the walls towards those sides. In Figure 17 the set of top and right bins are the ones corresponding to those directions and these are, in fact, the more discoloured ones and, thus, representative of lower muon rates for the month of September. It's from this analysis that we can infer that Figure 17 is representative of the walls surrounding the detector in September.

On a more detailed analysis, one can compare this result with the 2D model found in section 4 - review Figure 15. In general, the two are compatible. However, the right bottom area, that should represent one of the sides of the building closest to the detector in September, presents lower values in the 2D model, from 0.95 to 1.10, versus the ones on the "Overall view", going from 1.20 to 1.40. The reason for this incoherence has meanwhile been discovered. In the model, all the above ground floors were

[10]The fact that the bins are not punctual is misleading. They are referent to a single direction, meaning a single pair of azimuth and zenith angles, the latter being correspondent to the mean value of the interval to which the bin extends to. That being said those angles are still an approximation, given the already mentioned fact that we don't know exactly where the muon crossed the pad.

considered to be identical, which is not the case: on the last floor, for that region, the structure of the building in "non-existing", for it is where a Foucault Pendulum is located. That being said, in that region, the muons cross less matter than the one considered and, consequently, a larger quotient than the one found with this current version of the model would be expected. So, once the model is corrected in this aspect, we'll, possibly, get a total correspondence with the results.

### 5.2 Sides of the building

In order to make the results and the data from the 2D histogram easier we simplified it to 1D. Taking the June data and considering only the 4 values of $\phi$: $-90°$, $0°$, $90°$ and $180°$, one proceeds to study the differences in the total number of muons detected as a function of $\theta$ for each side of the building. Ultimately , the goal is to see which angles of incidence and which side of the building is more favorable for muons to go through. That is, for what trajectories more muons would be blocked by the matter of walls and ceilings resulting in fewer muons being detected. If for a certain angle $\theta$ and a certain side of the building the number of total events is bigger, we can conclude that muons with that trajectory travel across less matter. In the next figure we can see a graph with the relation in the rates for each side of the building between the months of August and September. The values in the vertical axis are the total number of events of September divided by the ones in August, considering the different acquisition time of the detector for each month. Since in September the detector was placed outside, we expect the number of events to be bigger because there is no damping from matter of the building. This graph not only proves that but it also allows to see how much the building affects the number of muons detected for each angle $\phi$ and $\theta$. We can also study more precisely how different number of walls and ceilings influence the detection, because this makes possible the comparison between different sides of the building ( diferent $\phi$'s for August) and the exterior.

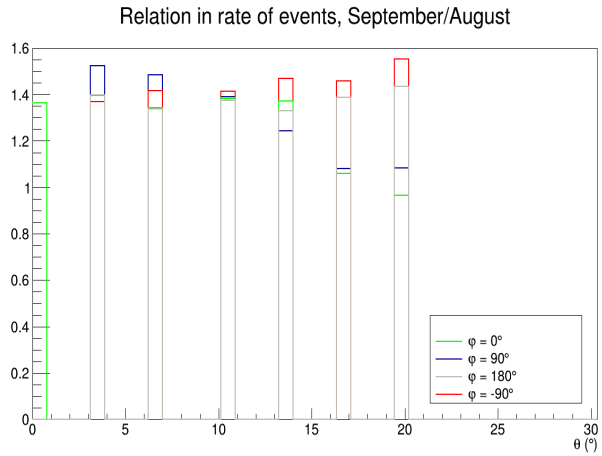


Figure 18: Quotient between the ratio of rates, in the 4 azimuth angles, that define the sides of the building, from September and August.

## 6 Results and Conclusions

With the analysis presented, we can conclude that further study of the detector is required, namely of what is originating its non-uniformity and equivalently the corepix efficiency pattern. Nonetheless, an attenuation of this same pattern has occurred and there is also to point out the positive that the increasing of the detector's average efficiency to $\sim 90\%$ represents.

About the results that characterize the building's interaction with the muons, there is to emphasize the confirmation of our assumptions towards the vertical transmission with Monte Carlo method and the $cos^2\theta$ dependency of the muons' directions distribution.

More importantly, one can assert with confidence that the building is visible on the two data study strategies adopted. When simply looking at the 2D histogram of the quotient between the data from August and September, the two walls that surround the detector during the second month are evident. The same inference applies to the 1D representation.

So, all in all, we can outline this project as having provided meaningful analysis from both, the detector study and the building muography, points of view.

## Acknowledgements

We would like to thank LIP for the opportunity of participating in the 2020 Summer Internships. Thank you for the great program that allowed our introduction to Particle Physics to be such a fulfilling learning experience. We would specially like to acknowledge the availability that every LIP member, from the investigators to the IT team, has continuously offered, namely during the workshops.
In particular, we want to express our great appreciation and gratefulness for the LIP investigators and our supervisors Raul Sarmento and Sofia Andringa, who have incessantly been at disposal to guide us through this project and to clear any doubts we encountered.

## References

[1] P. A. Zyla et al. (Particle Data Group), Prog. Theor. Exp. Phys. 2020, 083C01 (2020)

[2] K. Morishima et al., Nature 552, 386–390 (2017)

[3] https://goo.gl/maps/ojC19Udu5rVMgVqN7 (2020), [Online]

[4] P. Assis et al., in Proceedings of ICRC2017, Busan, South Korea, https://arxiv.org/abs/1709.09619 (2017), [Online]